

International Journal of Multidisciplinary Research and Growth Evaluation.



Performance Analysis of GaN-based H-bridge converter for high Power Conversion Systems

Snehalika 1*, Ranjeeta Patel 2, Chinmoy Kumar Panigrahi 3

- ¹ School of Electrical Engineering, KIIT Deemed to be University, Odisha, India
- ²⁻³ Senior Member, IEEE, School of Electrical Engineering, KIIT Deemed to be University, Odisha, India
- * Corresponding Author: Snehalika

Article Info

ISSN (online): 2582-7138

Volume: 04 Issue: 04

July-August 2023 Received: 01-07-2023 Accepted: 22-07-2023 Page No: 981-986

Abstract

This paper analyzes the performance analysis of Gallium Nitride (GaN)-based H-bridge converters for high Power Conversion Systems (PCS) such as electric vehicle charging systems. The same analysis is extended to a Si-based H-bridge converter for a comparative study. The objective is to perform a loss analysis of the H-bridge converter. The loss analysis is carried out for the conduction and switching losses of the device, anti-parallel diodes and high frequency link transformer (HFL). The performance study is done for the GaN-based and Si-based H-bridge converters operating at high switching frequencies ranging up to 300 kHz. The performance metrics of the 1 kW GaN based H-bridge have been analyzed and simulation is performed using LTspice XVII software. To verify the results, a 0.91 kW prototype operating at a frequency of 100 kHz is presented with Port-1/Port-2 voltages of 230/120 V respectively.

Keywords: Electric Vehicle (EV), Power Conversion Systems (PCS), high frequency link (HFL), Gallium Nitride (GaN), H-bridge

1. Introduction

Power electronic devices play a crucial role in converting large amounts of energy in industrial settings and serving as the foundation for high power conversion systems (PCS). Recently, there has been growing interest in gallium nitride (GaN) as an alternative to silicon-based power devices like conventional MOSFETs. GaN devices combine the advantages of both MOSFETs and IGBTs, offering the potential for higher switching frequencies, improved efficiency, and increased power density [1-3]. MOSFETs conducting characteristics vary significantly as they exhibit resistor-like conduction, resulting in conduction losses that increase exponentially with current. In this situation, the maximum drain current is limited by the power dissipation generated by R_{ds(on)}. MOSFETs are most commonly seen in low-voltage applications. MOSFETs have much higher R_{ds} values to resist high voltages, resulting in power dissipation limits and limiting current increases. Although MOSFETs with 600 V and 1000 V ratings are available, their current carrying capacity is often lower than that of GaN HEMTs, and the R_{ds} value is at least twice as high, if not more. In summary, GaN technology outperforms MOSFETs in terms of high-frequency, low-loss, and highvoltage applications. The composition and manufacturing processes of GaN HEMTs have been investigated in relation to various material compositions and manufacturing methods [4-5]. The reverse conduction voltage drop is principally connected with the gate-drive voltage, which distinguishes GaN HEMTs from traditional Si-based devices. In the literature, reverse conduction is rarely explored in depth. In [6], GaN device losses, including reverse conducting losses, are compared in the context of an Hbridge power converter operating a DC motor with various bipolar and unipolar modulation schemes. Nonetheless, [6] focuses primarily on always-on or always-off switching devices, ignoring the losses caused by the dead-band in a complementary modulated converter leg. Fig. 1 highlights key material properties of semiconductors, emphasizing SiC and GaN as leading options to replace Si [1, 7-8].

Scholars have been urged to employ wide band gap semiconductor (WBG) based switches instead of Si-based switches due to advancements in semiconductor material technology. Due to its high efficiency, high power density, and quick switching rates, GaN based converters can give increased performance in EV charging applications.

When compared to typical Si-based devices, GaN devices offer lower on-resistance and switching losses, resulting in improved efficiency and lower heat dissipation. Furthermore, quick switching rates enable faster reaction times, lowering charging time and enhancing total charging efficiency. Overall, GaN-based DC-DC converters outperform classic silicon-based devices in electric vehicle charging applications [9-11].

There are several control strategies present in the literature, such as single-phase-shift (SPS), double-phase-shift (DPS), triple-phase-shift (TPS), and extended-phase-shift (EPS). Amongst them, the SPS control strategy is found to be simple

and utilized here for the switching of H-bridge converter [12-13]

In this paper, performance analysis is carried out for the GaN-based H-bridge converter for high power conversion systems, and a high frequency link transformer is designed for carrying out the simulation and experimental study. The same analysis is carried out for a Si-based H-bridge converter and performance metrics are compared. The study is performed at both the discrete element level and the converter level. The analysis is carried out based on measured data in simulation and experiments.

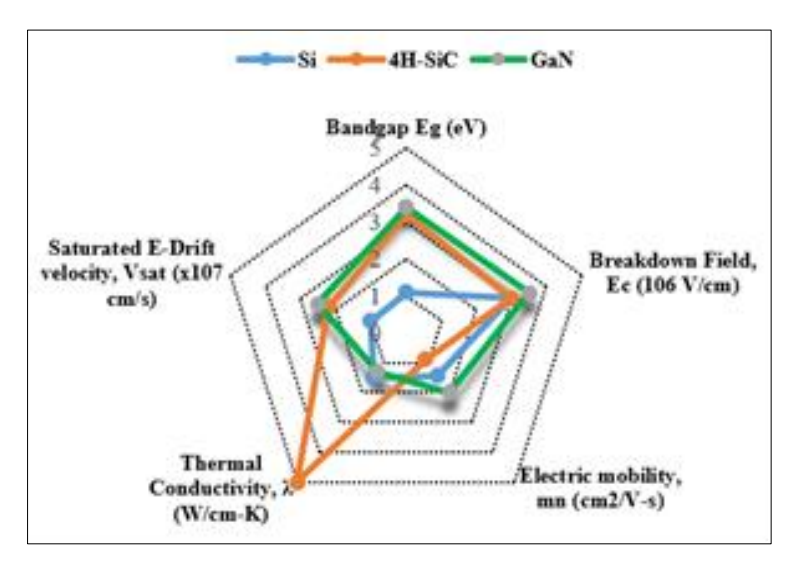


Fig 1: Overview of material properties of Si, SiC, and GaN [1]

In detail, this paper is organized as follows. Section II discusses the GaN-based H-bridge converter. Section III represents the design parameters of the GaN-based H-bridge converter. Section IV showcases experimental validation of the results provided in a simulation based analysis for the GaN-based H-bridge converter in Section III. Finally, Section V concludes the paper.

1. GaN-based H-Bridge converter

A general schematic of the H-bridge is illustrated in Fig. 2. The bridge consists of different components. The input bridge is powered by a dc input source $V_{\rm dc}$, and consists of switches S1-S4 and a high frequency transformer (HFT). The HFT is connected to the output terminals of the H-bridge. The H-bridge has been utilized for testing and performance analysis of the GaN-based converter. The same bridge can be utilized for comparative study of of the Si-based H-bridge.

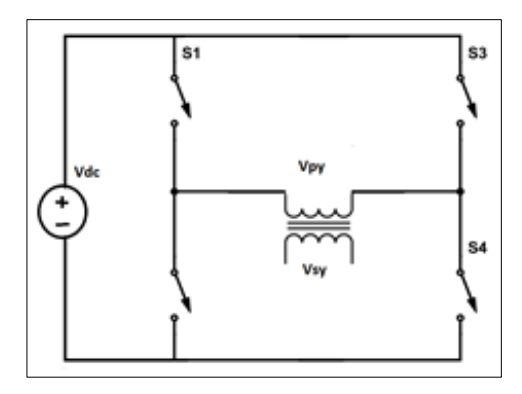


Fig 2: Schematic of the general configuration of H-bridge

In this paper, a 650 V GaN-HEMT from GaN Systems is compared with a 650 V n-channel MOSFET from STMicroelectronics. Table I lists the parameters of the two devices, GaN HEMT, and Si n-channel MOSFET.

Table 1: Parameters of DEVICES: GaN and Si

Device	GaN HEMT	n-channel MOSFET
Company	GaN Systems	STMicroelectronics
Part no.	GS66508T	STP8NM60
V _{DS} (V)	650	650
$I_{DS(max)}(A)$	30	8
$R_{\mathrm{DS(on)}}(\mathrm{m}\Omega)$	50	950
Q _G (Gate charge) (nC)	6.1	13
Operating Temperature (°C)	25	25
PCB Footprint (mm ²)	7×4.5	6.7×11.5

The rated voltages have been chosen same for the two devices in order to test them under same operating conditions. The rated value of $R_{\rm DS(ON)}$ of the GaN device is almost one-tenth of that of the n-channel MOSFET clearly indicating large conduction losses for the later under same operating conditions. The rated current differs by around 26.67%, which is due to device availability, as two devices with identical ratings are uncommon to find. The gate charge of the GaN devices is almost half of that of the Si device. The operating temperature is kept at 25 $^{\circ}{\rm C}$ for all operating conditions. The PCB footprint indicates a decrease in the component size of the GaN device.

2. Simulation Results and Analysis

To validate the GaN-based H-bridge converter extensive

simulation is carried out using the LTSpice XVII simulation tool. The GaN-based and Si-based converter efficiency will be evaluated in terms of the total power losses. This requires a detailed analysis of each component of the total losses, which is discussed in this section.

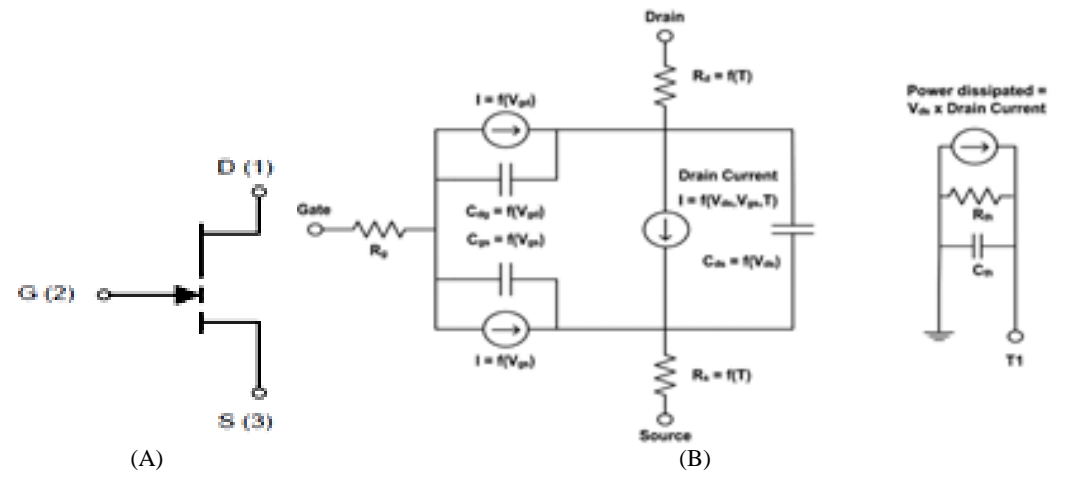
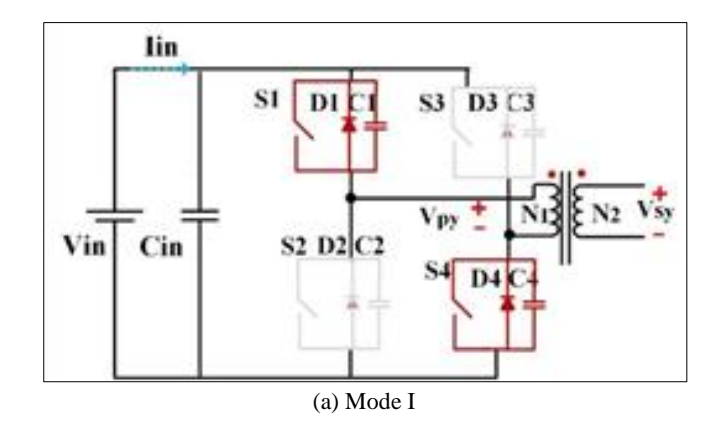


Fig 3: (a) Gallium Nitride HEMT circuit Symbol and (b) Equivalent sub-circuit of HEMT model by GaN Systems

Fig. 3 displays both the circuit symbol and the functional block diagram of the sub-circuit being used. This sub-circuit is represented by a voltage-controlled current source, which takes into account the gate to source voltage (V_{gs}), drain to source voltage (V_{ds}), and temperature variations. The model also includes the gate resistor (R_g), a temperature-dependent drain resistor (R_d), and a temperature-dependent source resistor (R_s). Additionally, the model incorporates voltage-dependent parasitic capacitors ^[14].



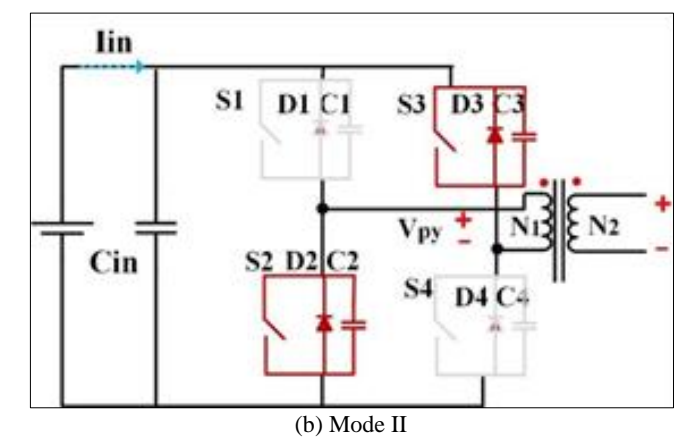


Fig 4: Mode of operation of the H-bridge converter in different modes

The entire operation of the H-bridge can be divided into two modes as presented in Fig. 4. The Mode I indicates conduction of S1 and S4 providing a positive voltage at the primary of the transformer. The Mode II indicates conduction of S2 and S3 providing a negative voltage at the primary of the transformer. The analysis focused on determining the conduction loss, switching loss, and total loss, as these properties were deemed necessary for the loss analysis.

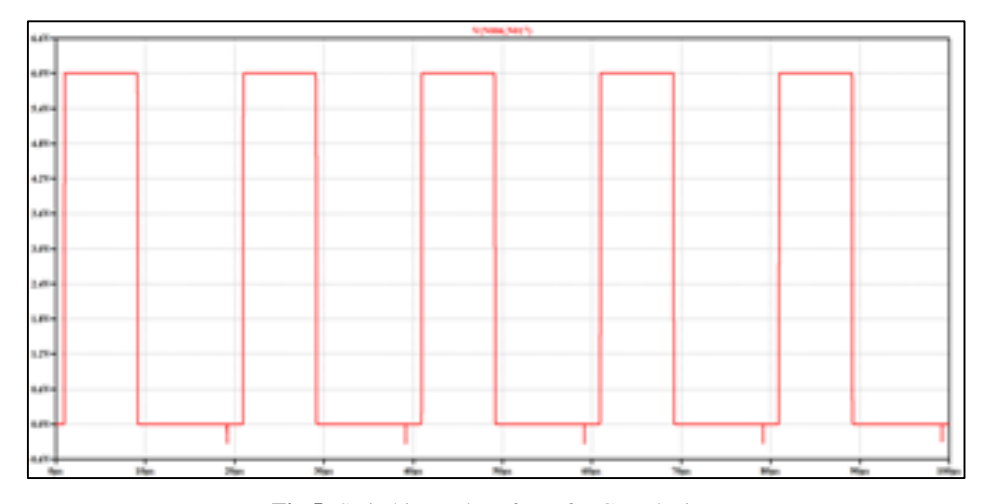


Fig 5: Switching pulse of 6 V for GaN devices

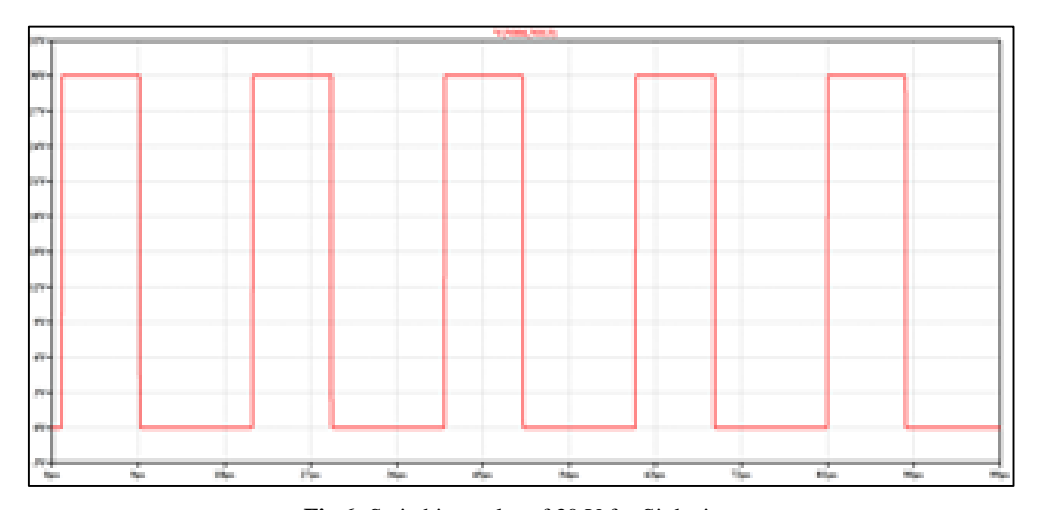


Fig 6: Switching pulse of 30 V for Si devices

A. Power Losses in Semiconductor Devices

The total losses that developed in semiconductor power devices can be divided into conduction and switching losses. The assessment of conduction losses in semiconductor devices can be performed by analyzing their current waveform, ON-state voltage, and conducting interval. The calculation of power transistor conducting losses can be determined by using (1).

$$P_{C} = I_{rms}^{2} R_{DS(ON)}$$
 (1)

Where Irms and RDS(ON) are the rms value of switch current and drain to source resistance respectively. The switching losses, Psw of devices as a function of varying switching frequency, ranging from 50 kHz to 300 kHz can be calculated using (2) while maintaining a constant duty cycle of 0.5.

$$P_{SW} = (1/2). V_{DS}. I_{DS}(t_{on(s)} + t_{off(s)}). f_{S}$$
 (2)

Where, f_{S} is the switching frequency, V_{DS} and I_{DS} are the drain to source voltage and drain to source current of the switch respectively. The $t_{on(s)}$ and $t_{off(s)}$ for the switches can be calculated using (3) and (4) respectively.

$$t_{on(s)} = (t_{D_{on}} + t_{r})$$
(3)

$$t_{off(s)} = (t_{D_{off}} + t_f) \tag{4}$$

indicates the summation of turn-on delay, $^{t_{D_{on}}}$ and rise time, $^{t_{r}}$ and $^{t_{off}(s)}$ indicates the summation of the turn-off delay, $^{t_{D_{off}}}$ and fall time, $^{t_{f}}$ for the GaN HEMT and Si MOSFET taken from the datasheets provided by the manufacturer in $^{[14,15]}$.

The total losses, P_{ST} of the switching devices can be determined using (5).

$$P_{ST} = P_C + P_{SW} \tag{5}$$

The switching losses, PST were computed for one switch and is then multiplied for four number of switches used in H-

bridge) to obtain the total losses of the converters.

B. Power Losses in Diodes

Power losses can be evaluated for diodes based on the measurement of forward voltage drop and current flowing in the device. The H-bridge incorporates four diodes D1-D4. The conduction losses, Poof the diodes can be calculated using (6).

$$P_{CD} = \frac{1}{T_{S}} \int_{t_{1}}^{t_{2}} I_{DS}. V_{f} dt$$
 (6)

Where, T_S is the time period, V_f and I_{DS} are the forward voltage drop and drain to source current of the diode respectively. The losses are calculated over a time period T_S from t_1 to t_2 .

C. Transformer losses

The transformer consists of majorly two losses, the iron loss, and the copper loss. The iron loss occurring in the magnetic core of the transformer is also known as the fixed loss. The loss can be computed using (2.7).

$$P_{iron} = V_c. K_1. f_s^{\alpha_c}. B^{\beta_c} + K_2. f_s^2. B^2$$
 (7)

Where, V_c is the core volume, f_S is the switching frequency,

B is the flux density K_1 , K_2 , α_c , and β_c are constants that can be determined with the help of the core data sheet. The iron losses of the transformer depend on the magnetic flux, the frequency, the core volume, and the voltage waveform available at the transformer.

The copper loss in the winding of the transformer can be calculated using (8).

$$P_{copper} = I_{rms}^2 R_{eff}$$
 (8)

Where, where Irms is the rms value of the transformer current and his the total effective resistances of the primary and secondary windings, referred to as the primary side of the transformer.

D. Total losses

The total losses, Ptotal on the H-bridge can be computed by summation of the losses on the semiconductor switches, diodes, and transformer losses. The same can be computed using (2.9).

$$P_{\text{total}} = P_{\text{ST}} + P_{\text{CD}} + P_{\text{iron}} + P_{\text{copper}}$$
(9)

The major percentage of total losses incurred in the H-bridge circuit is due to the semiconductor devices. As the conduction and switching losses are the major losses in a semiconductor device, they have been discussed in detail in th next section. The conduction losses concerning the duty cycle varied from 0.1 to 0.8 for a constant switching frequency of 50 kHz and is presented in Fig. 7. The switching losses, P_{SW} were computed for one switch and then multiplied for four switches (used in DAB) to obtain the total losses of the converters and is presented in Fig. 8. The total losses, P_{total} of GaN HEMT and Si-MOSFET is presented in Fig. 9.

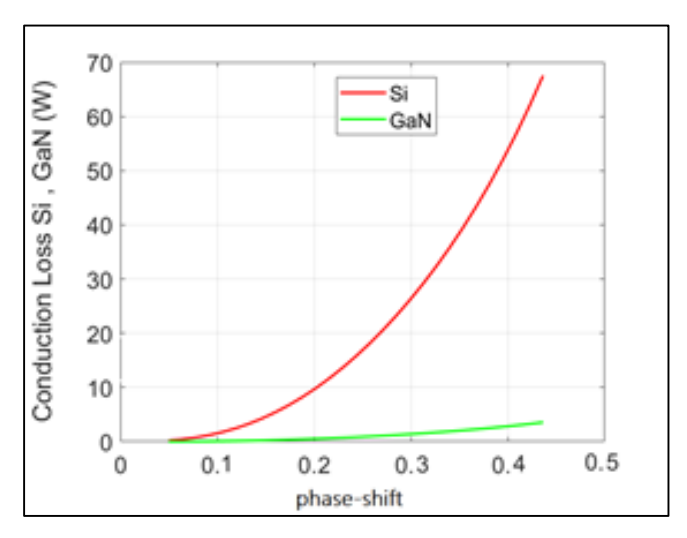


Fig 7: Conduction losses vs phase-shift at 50 kHz

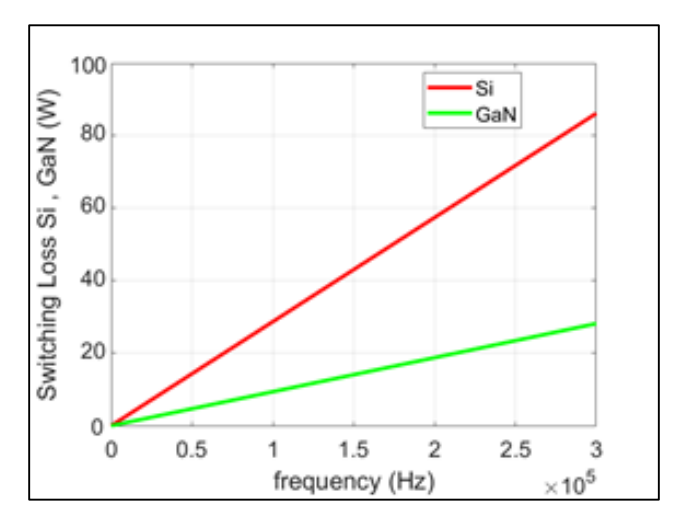


Fig 8: Switching losses vs Frequency

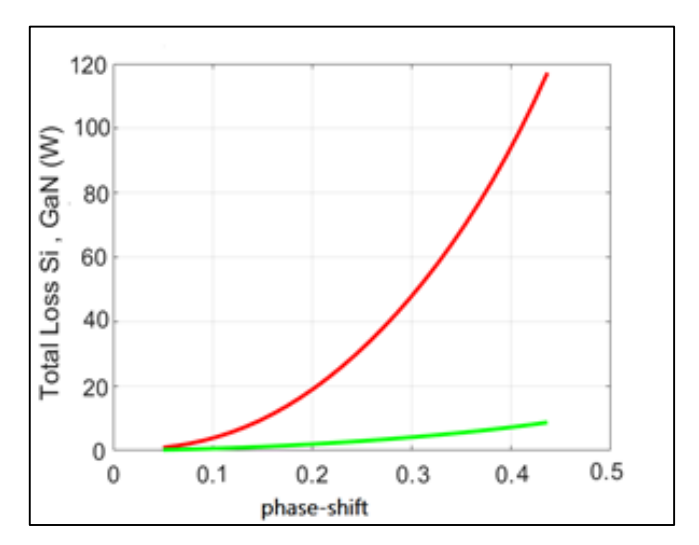


Fig 9: Total losses vs phase-shift at 50 kHz

The conduction losses have been plotted with respect to the phase-shift, the switching losses are plotted with respect to the frequency and the total losses are plotted with respect to phase-shift at a constant switching frequency of 50 kHz respectively in figures Fig. 7, Fig. 8 and Fig. 9. The plots are computed for both the devices, Si in red and GaN in green. Equations (1)- (9) is utilized to calculate the losses in the Sibased H-bridge converter and GaN-based H-bridge converter. All the losses are compared for both the devices and plotted on the same axis in figures Fig. 7, Fig. 8 and Fig. 9. The below plots in figures Fig. 7, Fig. 8 and Fig. 9 clearly indicates the rise of losses with an increase of phase-shift values and an increase of frequency values for the Si-based H-bridge converter compared to the GaN-based H-bridge converter. The obtained losses are clearly higher of a Sibased compared to a GaN-based converter.

Conclusion

A simulation analysis on the characteristics of Silicon (Si) and Gallium Nitride (GaN) devices in high-power conversion systems is done. A high frequency link ensures reduction in volume, weight and cost of the circuit. The conduction losses of the Si-based H-bridge increased substantially with an increase in phase-shift values from 10 W to 70 W as can be seen in Fig. 7. The GaN-based H-bridge incurred losses below than 10 W for all operating conditions of phase-shift. As plotted in Fig. 8, the switching losses significantly increased beyond 80 Was the switching frequency increased to 275 kHz for the Si-based H-bridge. The switching losses for GaN-based H-bridge remain under 30 W for all values of switching frequency. The total losses plotted in Fig. 9 indicates clearly that beyond the operating frequency of 10 kHz, the Si-based H-bridge incurs significantly higher losses than the GaN-based H-bridge with phase-shift being varied from 0 to 0.5. It is observed that the conduction and switching losses in GaN-based H-bridge is significantly less than the Sibased H-bridge circuit at all operating conditions. It is clearly observed that the GaN devices are a preferable choice over

the Si devices for high frequency range operation beyond 10 kHz. The analysis is done for eight switches in order to implement the GaN devices in the Dual Active Bridge circuit for the future work.

References

- 1. Millan J, Godignon P, Perpina X, Perez-Tomas A, Rebollo J. A survey of wide bandgap power semiconductor devices. IEEE Transactions on Power Electronics. 2014;29(5):2155-63. doi: 10.1109/TPEL.2013.2268900.
- 2. Peng K, Eskandari S, Santi E. Characterization and modeling of a gallium nitride power HEMT. IEEE Transactions on Industrial Applications. 2016;52(6):4965-75. doi: 10.1109/TIA.2016.2587766.
- 3. Mitova R, Ghosh R, Mhaskar U, Klikic D, Wang MX, Dentella A. Investigations of 600-V GaN HEMT and GaN diode for power converter applications. IEEE Transactions on Power Electronics. 2014;29(5):2441-52. doi: 10.1109/TPEL.2013.2286639.
- 4. Mantooth HA, Peng K, Santi E, Hudgins JL. Modeling of wide bandgap power semiconductor devices Part I. IEEE Transactions on Electron Devices. 2015;62(2):423-33. doi: 10.1109/TED.2014.2368274.
- 5. Li K, Evans PL, Johnson CM. Characterisation and modeling of gallium nitride power semiconductor devices dynamic on-state resistance. IEEE Transactions on Power Electronics. 2018;33(6):5262-73. doi: 10.1109/TPEL.2017.2730260.
- Lee W, Han D, Choi W, Sarlioglu B. Reducing reverse conduction and switching losses in GaN HEMT-based high-speed permanent magnet brushless DC motor drive. In: 2017 IEEE Energy Conversion Congress and Exposition (ECCE 2017); 2017 Jan. p. 3522-8. doi: 10.1109/ECCE.2017.8096628.
- 7. Santi K, Peng K, Mantooth HA, Hudgins JL. Modeling of wide-bandgap power semiconductor devices Part II. IEEE Transactions on Electron Devices. 2015;62(2):434-42. doi: 10.1109/TED.2014.2373373.
- 8. Peng K, Eskandari S, Santi E. Characterization and modeling of a gallium nitride power HEMT. IEEE Transactions on Industrial Applications. 2016;52(6):4965-75. doi: 10.1109/TIA.2016.2587766.
- 9. Esteban D, Serra FM, De Angelo CH. Control of a DC-DC dual active bridge converter in DC microgrids applications. IEEE Latin America Transactions. 2021;19(8):1261-9. doi: 10.1109/TLA.2021.9475856.
- Snehalika, Das S, Patel R, Panigrahi CK. GaN-based isolated bi-directional DC-DC converter for high load current application. In: 2022 IEEE Delhi Section Conference (DELCON); 2022. p. 1-7.
- Snehalika, Patel R, Panigrahi CK, Rathore AK. High-power isolated bidirectional three-port DC-DC converter for Level-1 and Level-2 charging. In: 2022 IEEE 2nd International Conference on Sustainable Energy and Future Electric Transportation (SeFeT); c2022 Hyderabad, India. p. 1-6.
- Yan Y, Gui H, Bai H. Complete ZVS analysis in dual active bridge. IEEE Transactions on Power Electronics. 2021;36(2):1247-52. doi: 10.1109/TPEL.2020.3011470.
- Hannan MA, Hoque MM, Hussain A, Yusof Y, Ker PJ. State-of-the-art and energy management system of lithium-ion batteries in electric vehicle applications: Issues and recommendations. IEEE Access.

- 2018;6:19362-78. doi: 10.1109/ACCESS.2018.2817655.
- 14. GaN Systems. LTspice Model User Guide. 2017. p. 1-7.
- GaN Systems. GS66508T Top-Side Cooled 650 V E-Mode GaN Transistor Preliminary Datasheet. c2020. Rev 200402. p. 1-16. Available from: https://GaNsystems.com/wp-content/uploads/2020/04/GS66508T-DS-Rev-200402.pdf.